Journal of Materials Chemistry A

ARTICLE

On the use of surfactants for improving nanofiller dispersion and piezoresistive response in stretchable polymer composites

Received 00th January 20xx,

Accepted 00th January 20xx

DOI: 10.1039/x0xx00000x

www.rsc.org/

P. Costa*[a,b], A. Maceiras[c], M. San Sebastián[c], C. García-Astrain[c], J.L. Vilas[c,d], S. Lanceros-Mendez[c,e]

Conducting polymer composites are increasingly investigated for the development of piezoresistive materials for sensor applications due to their outstanding electromechanical properties. In this work, the effect of different surfactants on the piezoresistive response of triblock copolymer styrene-butadiene-styrene (SBS)/carbon nanotubes (CNT) composites was studied. Surfactants act as dispersing agents for CNT decreasing the size of agglomerates. The use of different surfactants such as Triton-X100 (TX-100), cetyltrimethylammonium bromide (CTAB) and sodium dodecylbenzenesulfonate (SDBS) affects the percolation threshold as well as the mechanical and piezoresistive properties of the composites. TX-100 decreases the mechanical response and electrical conductivity of the polymer composites, leading also to low piezoresistive response. CTAB and SDBS decrease the size of the agglomerates while maintaining their electrical conductivity up to 4 wt% CNT. Moreover, these composites present improved piezoresistive response with GF values up to 3 and deformations up to 10%, similar to the behaviour of commercial sensors with improved filler dispersion within SEBS polymer and promoting the use of novel range of printable methods.

1. Introduction

Smart materials based on polymer composites have demonstrated their potential for a broad variety of applications ranging from industrial to advanced biomedical applications [1-3]. The simple processing, flexibility and biocompatibility of the polymer matrices coupled with the excellent mechanical, electrical and chemical properties of the nanofillers are some of the reasons for the increasing use of these materials [1, 2, 4]. In the last decades, efforts have been devoted to achieving high performance multifunctional composites, while preserving the mains features of the polymeric matrix [1, 5].

Among the vast variety of smart composites, piezoresistive materials are particularly interesting due to the large number of potential polymer/nanofiller combinations and their applicability as force and deformation sensors [5, 6]. These different combinations allow the fine-tuning of material properties for specific applications [4, 7]. Conductive fillers such as carbon nanotubes, carbon nanofibers or graphene allow the tailoring of the composite electrical, mechanical, thermal

a- Center of Physics, University of Minho, 4710 - 057 Braga, Portugal
b- Institute for Polymers and Composites (IPC), University of Minho, 4800-058 Guimarães, Portugal
c- BCMaterials, Basque Center for Materials, Applications and Nanostructures, UPV/EHU Science Park, Barrio Sarriena s/n, 48940 Leioa, Spain
d- Departamento de Química Física, Facultad de Ciencia Y Tecnología, Universidad del País Vasco/EHU, Apdo. 644, Bilbao, Spain
e- IKERBASQUE, Basque Foundation for Science, 48013 Bilbao, Spain
**Corresponding author: pcosta@fisica.uminho.pt*

and electromechanical properties by varying their size, aspect ratio or surface area, among others [1].

Carbon nanotubes (CNT) result particularly interesting for the development of conducting polymers and piezoresistive sensors due to their excellent electrical and mechanical properties [8, 9]. Moreover, CNT lead to lower percolation threshold than other fillers, a key issue in the development of piezoresistive composites. Usually, when a strain is applied to the composite, the largest electro-mechanical response -variation of the electrical resistivity upon mechanical deformation- is observed near the percolation threshold [10]. The addition of nanofillers slightly increases the electrical conductivity of the composite up to a certain extent, when the percolation threshold is reached, and the electrical conductivity increases by several orders of magnitude [11]. The conductive networks formed by CNT within the polymer matrix determine the electrical properties of the composites and when a strain is applied, variations of the conductive network occur, attributed to loss of contact between fillers, tunnelling [11] or hopping [12] effects in neighbouring fillers. The conductivity relies on the interactions between nearby conductive nanofillers and, thus, these conductive networks depend on CNT dispersion [11, 12].

To develop piezoresistive composites for large deformation applications, soft polymers such as thermoplastic elastomers (TPE) are an interesting option as they combine the mechanical properties of rubbers (elastic recovery after large applied deformations) and the ease of processability of thermoplastics [13]. The TPE tri-block copolymers styrene-butadiene-styrene (SBS) haven been intensively used in industrial applications due to their excellent properties such as tensile strength and abrasion resistance. However, SBS is sensitive to degradation mainly due to the elastomeric polybutadiene (PB) phase [13]. To circumvent this drawback, the saturation of butadiene segments in SBS with ethylene-butadiene segments results in a new type of TPE, styrene-ethylene-butadiene-styrene (SEBS) [13]. SEBS shows similar properties than SBS but with an improved oxidative stability. Further, the elastic properties are improved by decreasing the amount of butadiene phase.

As previously mentioned, the piezoresistive response in polymer composites depends on several parameters such as the nanofiller content and dispersion, affecting the electrical and mechanical properties, signal degradation over time, and sensibility of these materials [14, 15]. One of the main issues that needs to be faced during composite preparation is the agglomeration of CNT, in particular in aqueous solutions, due to strong van der Waals interactions between the nanofillers [16]. To achieve a uniform and stable dispersion, a strong interfacial interaction/wetting between CNT and the polymer matrix is required [17]. Mechanical approaches involve ultrasonication and stirring of CNT, steps that are usually time-consuming [18]. On the other hand, the chemical functionalization of CNT can improve their dispersion but can also deteriorate the properties of the nanofillers [17]. For this reason, the use of dispersants during solution mixing represents a suitable alternative to overcome CNT aggregation problems [17, 19]. In this way, the non-covalent interactions stablished rarely damage the structure of CNT preserving the inherent π-bonds and their electrical properties [20]. The dispersion of CNT in water using surfactants results from the decrease of van der Waals interactions between CNT due to their hydrophobic tails that wrap CNT via non-covalent bonding and their hydrophilic part that provides aqueous solubility and electrostatic repulsion [21, 22]. Thus, a thermodynamic equilibrium between repulsive and attractive forces is created and regulates the dispersion or aggregation of CNT. Factors such as alkyl chain length, charge concentration and adsorption of other

chemicals on the coated CNT influence the adsorption of surfactants to the surface of the nanofillers [23].

The dispersion ability and the stability of the dispersions depend on the type and nature of surfactant [24]. For example, the cationic surfactant cetyltrimethylammonium bromide (CTAB) can suspend the CNT better than an anionic surfactant such as sodium dodecyl sulphate (SDS), due to their longer alkyl chain, and therefore, would lead to stronger hydrophobic interactions between the CNT and CTAB [25]. On the other hand, anionic surfactant sodium dodecyl benzene sulfonate (SDBS) contributed to a better dispersibility and electrical conductivity of CNT than SDBS, CTAB or other surfactants [26]. Triton, a nonionic surfactant containing a branched tail, promotes the CNT dispersion due to strong hydrophobic attraction between the solid surface and the tail group of surfactant [20]. Thus, it is crucial to find the appropriate surfactant for the suitable dispersion of CNT within a given polymer matrix. The filler dispersion is particularly relevant when the composite is prepared in the form of inks for printed sensors [5], area which is receiving an increasing interest for wearables and large area applications [27, 28]. Achieving a homogeneous solution for inks preparation is a key parameter to easy printing processes.

In this work, the effect of using three different surfactants, namely CTAB, SDBS and Triton X-100 (cationic, anionic and nonionic, respectively), over the mechanical, electrical and piezoresistive properties of CNT/SEBS composites is presented. In view of the increasing interest of those materials for application as smart inks for printing technologies such as spray, screen or inkjet printing [27, 28], where dispersion and size of the clusters are critical parameters, controlled and stable CNT clusters are needed [5].

2. Experimental

2.1. Materials

The elastomeric polymer used is a biocompatible thermoplastic elastomer Calprene CH-6120, a Styrene-Ethylene/Butylene-Styrene (SEBS) triblock copolymer with a ratio of Ethylene-Butylene/Styrene of 68/32 and a molecular weight of 245.33 g/mol, provided by Dynasol Elastomers. Multi-walled carbon nanotubes (CNT) were supplied by Nanocyl: reference NC7000 with length of 1.5 µm and outer mean diameter of 9.5 nm and 90% of purity. The solvent used was cyclopentyl methyl ether (CPME) from Carlo Erba with a density of 0.86 g/cm^3 at 20 ºC. CPME is a greener hydrophobic ether solvent. Three surfactants were used to prevent CNT agglomeration; sodium dodecylbenzenesulfonate (SDBS, molecular weight of 348.48 g/mol and a concentration ≤100%), cetyltrimethylammonium bromide (CTAB, 364.45 g/mol and a concentration ≤100%) and Triton-X100 (TX-100, a concentration between 90 and 100) from Sigma-Aldrich and they were used as purchased.

2.2. CNT/SEBS composites preparation

CNT/SEBS composites were prepared with 0, 0.25, 1, 2, and 4 weight percentage (wt%) of CNT. Firstly, CNT and the surfactant were mixed in a 2:1 ratio CNT/surfactant (for three different surfactants) in CPME (12 ml) and put in an ultrasound bath (ATU, Model ATM40-3LCD) for 3 h between 25 to 35 ºC for homogeneous dispersion of the CNT in the solvent. To understand the surfactant effect in CNT dispersion, for CNT/SEBS composite with 2 wt% CNT, the ratio was varied for 1:1 and 1:2 CNT/surfactants contents, using similar processing conditions. After dispersion of the CNT was achieved, SEBS was added with a polymer/solvent ratio of 1:6 (grams of polymer to mL of solvent) and the solution was magnetically stirred at room temperature (≤ 35 ºC) until complete dissolution of the SEBS. The

CNT/SEBS films were then prepared by solution casting on a clean glass substrate and dried at room temperature for 24 h until total solvent evaporation. The film thickness was between 100 and 200 µm.

Table 1- Experimental conditions for CNT/SEBS composites preparation with the different surfactants. The CNT/surfactant ratio is 2:1 wt% for composites with different CNT contents. Composites with 2 wt% CNT have been prepared with different CNT/surfactant ratio.

CNT (wt%)	CNT/Surfactant		
	TX-100	CTAB	SDBS
0	2:1		
0.25	2:1		
1	2:1		
2	2:1		
	1:1		
	1:2		
4	2:1		

2.3. Characterization of the samples

The morphology of the polymer was analysed by Scanning Electron Microscopy (SEM) using a Hitachi S-4800 field emission SEM at an accelerating voltage of 5 kV with magnifications of 2 000×, 10 000× and 50 000×.

Fourier transformed infrared, FTIR, spectra were recorded at room temperature in a Jasco FT/IR-4100 equipment in the attenuated total reflectance mode (ATR) from 600 to 4000 cm^{-1}, after 64 scans and with a resolution of 4 cm^{-1}.

Thermogravimetric analysis (TGA) was performed in a METTLER TGA/SDTA 851 thermobalance. The materials (about 5-10 mg) were heated from room temperature to 900 °C at a heating rate of 10 °C/min under a nitrogen atmosphere.

Mechanical measurements were performed with a universal testing machine (Shimadzu model AG-IS) at room temperature, in tensile mode, with a load cell of 500 N. Rectangular shape samples with area of 10 x 8 mm (height x width) and thickness from 100 to 200 µm (measured with digital micrometer Fischer Dualscope 603-478) were evaluated at a test velocity of 2 mm/min.

Dielectric measurements were performed with a Quadtech 1929 Precision LCR meter. Measurements were carried out in the parallel capacitor approach with 5 mm diameter Au contacts previously sputtered under vacuum in both sides of the samples with a Polaron SC502 sputter coater. The capacity and the dielectric losses were obtained at room temperature in a frequency range between 100 Hz to 1 MHz and the dielectric constant was obtained from the capacity measurements considering the geometrical characteristics.

The d.c. electrical resistivity was evaluated from the I-V characteristic curves obtained by applying voltages between -10 V to +10 V and measuring the current, with an automated Keithley 487 picoammeter/voltage source. The electrical resistance of the films (in volume) was calculated from the slope of the current-voltage curves, the measurements being collected from the 5 mm diameter Au contacts previously deposited as mentioned. The electrical conductivity (σ) of the material was calculated by:

$$\sigma = \frac{t}{R.A} \quad (1)$$

where R is the resistance, A is the area of the electrodes and t is the thickness of the sample.

The piezoresistive measurements were performed in real time by measuring the electrical resistance using the Agilent 34410A multimeter with the samples being subjected to applied mechanical strain in a universal testing machine (the same used in mechanical tests with a load cell of 50 N). Silver paint (from Colloidal Silver Paint from Ted Pella, Inc.) was used to paint the electrodes that are placed between the claws of the machine to avoid electric noise or deformation during the tests.

The piezoresistive behaviour was measured for strains from 1 to 10% and for 100 cycles in order to evaluate the electrical stability of the

composites. All measures were performed at 5 mm/min in samples with 10×8 mm (height × width) of area and near 150 µm of thickness. The piezoresistive performance was calculated by the Gauge Factor (*GF*) - equation 2 - at several strains for the surfactant-CNT/SEBS composites with 2 and 4 wt%. The *GF* was quantified by:

$$GF = \frac{dR/R}{\varepsilon_l} = \frac{d\rho/\rho}{\varepsilon_l} + (1 + 2\upsilon) \quad (2)$$

where *dR/R* is the relative resistance variation with applied strain, ε_l is relative strain and υ is the Poisson coefficient. The change in resistance is due to both the geometric effects (1+2v) and the fractional change in resistivity ($d\rho/\rho$) of the material with strain [29]. The Poisson coefficient for elastomeric materials is around 0.5 and the $1 + 2\upsilon$ factor is close to 2 for these kind of materials [29]. Piezoresistive performance of the composites with GF values below 2 can be attributed to the geometric factor ($1 + 2\upsilon$). Materials with GF larger than 2, above the geometric factor contribution, show an intrinsic resistivity variation affecting the piezoresistive sensibility.

3. Results and Discussion

3.1. Composite morphology

The influence of materials composition, including the addition of the surfactant, on the morphology of the composites was evaluated. SEM images (Figure 1) show the composites with 2 wt% CNT, with and without the different surfactants (Triton X-100, SDBS and CTAB) and different surfactant/CNT ratios.

CNT/SEBS composites without surfactant (Figure 1A) present some agglomerates with average diameter of 5 µm diameter, as already reported for similar composites [29] or even using different polymers and solvents [27]. The size of the clusters when using a surfactant as dispersion agent decreases and a better CNT dispersion is achieved, as can be seen in images at higher magnifications (Figure 1 B, C and D).

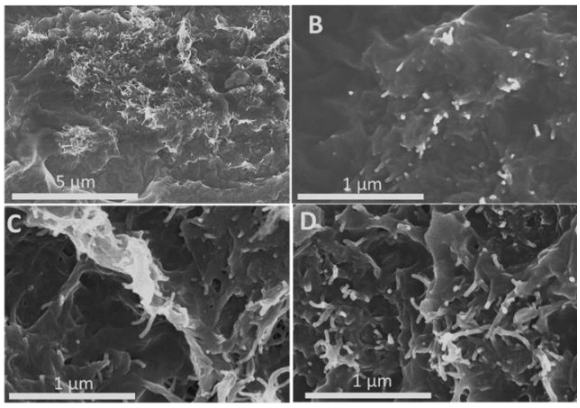

Figure 1 SEM images for CNT/SEBS composites with 2 wt% of CNT. Composites without surfactant A) and with surfactant, in a 1:1 ratio of CNT/surfactant, for B) TX-100, C) CTAB and for D) SDBS. The magnification used is 10 000x and 50 000x.

The surfactant effect is similar for the different surfactants employed (Figure 1B to D and supporting information in Figure S1) and no relevant differences in CNT dispersion were observed for 1:1 and 1:2 CNT/surfactant ratios, despite the slightly better dispersion found for the 1:2 ratio (Figure S2). Both small clusters and individually dispersed CNT are observed in composites using TX-100, CTAB and SDBS surfactants. Therefore, surfactant improves the dispersion of CNT when compared to composites without surfactant, while the ratio CNT/surfactant does not have a relevant influence on the nanofiller dispersion. The percolation threshold in composites depends on the CNT dispersion, where the clusters size distribution in composites strongly influences both maximum conductivity and percolation threshold [30, 31]. The loosely entangled and uniformly distributed CNT agglomerates present lower percolation threshold and larger maximum conductivity compared to tightly entangled CNT agglomerates; individual CNT dispersion can even lead to quite large percolation thresholds [30]. The use of surfactants does not seem to affect the structure of CNT, in agreement with [32]. Nadler et al. reported that ultrasonication does not completely separate the

nanofillers and the adsorption of surfactant prevents their reaggregation. Moreover, the gaps produced by ultrasonication at the end of the bundles can propagate until an individual nanotube is isolated when using surfactants [33]. The smaller clusters of CNTs are interesting for novel sensors devices fabricated by printing technologies, in which ink characteristics and printing technology are critical for suitable device performance.

3.2 Physico-chemical characterization

The FTIR spectra for the different CNT/SEBS composites with TX-100 surfactant are presented in Figure 2.

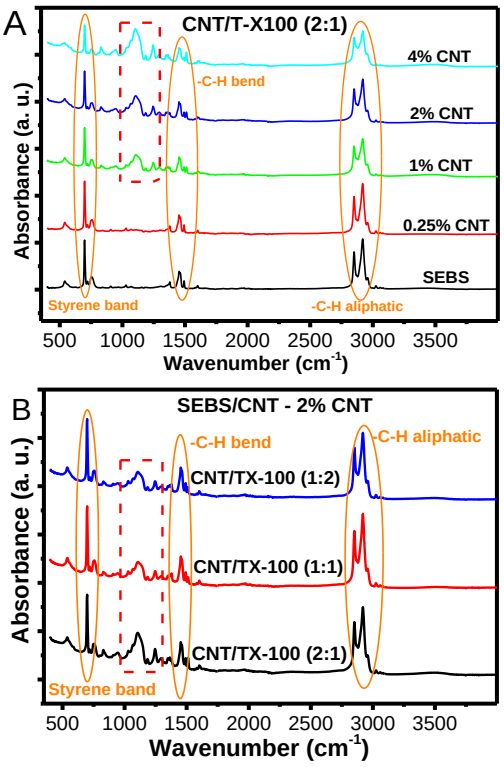

Figure 2 FTIR spectra for the different composites as a function of the CNT content (A) and ratio of CNT/surfactant (B) for the TX-100 surfactant.

The typical absorption bands of SEBS can be identified at 699 cm^{-1} for the =C-H bending vibration of the aromatic ring of the styrenic block and at 2850 and 2925 cm^{-1} for the C-H asymetric and symetric stretching vibrations of the -CH_2- of the ethylene/butylene block chain, respectively [29, 34].

After the CNT and surfactant addition no significant changes were observed in the spectra for composites prepared with SDBS or CTAB (Figure S2). However, the spectra of the composites prepared using TX-100 show absorbtion bands between 1100-1350 cm^{-1} for composites with 1 wt% CNT or higher, attributed to C-O stretching vibration of TX-100 surfactant attached on the CNT surface [9, 20]. The band intensities decrease when decreasing the CNT/surfactant ratio in these composites (Figure 2B), as reported in [20].

3.3 Thermal Properties

The thermal degradation of the composites was studied by thermogravimetric analysis (TGA). Figure 3A shows the TGA curves of pristine SEBS and CNT/SEBS composites of varying surfactant and filler content.

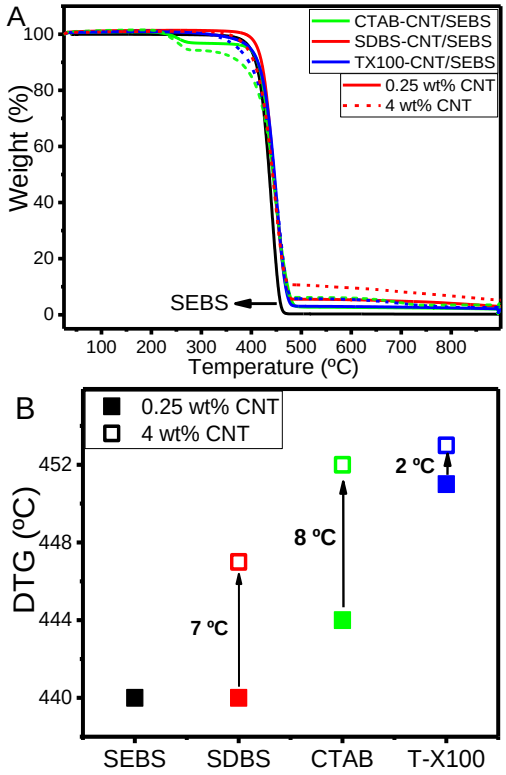

Figure 3 TGA spectra of the SEBS and composites with 0.25 and 4 wt% of CNT. In composites different surfactants were used (SDBS, CTAB or TX-100) with a CNT/surfactant 2:1 relation.

The degradation of SEBS starts at 370 °C and a weight loss of 99% is observed at 470 °C. When using CTAB as surfactant, an additional degradation step corresponding to CTAB degradation is observed in the thermogram and the degradation starts earlier, near 250 °C [35]. The composites show similar degradation pattern than SEBS. The maximum degradation temperatures for each type of composite, determined from the derivative thermogravimetric curve (DTG), are represented in Figure 3B. An increase in the degradation temperature was observed for the composites prepared using CTAB and TX-100 as surfactants with the lowest CNT content. In the case of using SDBS, similar degradation temperature was observed when compared with pristine SEBS. In all cases, the addition of higher amounts of CNT resulted in an increase of the degradation temperature of the composites. In this way, surfactant and CNT content increase slightly the DTG, giving some thermal stability to the composites. The thermal behaviour analysed by DSC do not shows observable distinct behaviour compared several surfactants or contents in composites (data not shown).

3.3 Mechanical Properties

The mechanical properties of the CNT/SEBS composites with different surfactants and filler contents are presented in Figure 4 for TX-100 surfactant. For CTAB and SDBS the stress-strain curves are similar to pure SEBS (with maximum strain between 400% to 800%) and are shown in the Figure S2. For composites with 2 wt% CNT (for CTAB and SDBS surfactant), the CNT/surfactant ratio was varied from 1:1, 1:2 or 2:1 to study the surfactant effect in composites, but no effect in mechanical properties was observed. The mechanical properties of the soft component in the copolymer (ethylene/butylene) is not affected by small contents of CNT. For composites with TX-100 surfactant, due to their mechanical properties with increase filler (and surfactant) content this step was not necessary. In composites with carbonaceous nanofillers the surfactant can act as a bridge between the carbon nanofillers and the rubber matrix, resulting in improved compatibility and wettability of the nanocomposites[9].

The stress-strain response of the SEBS polymer shows typical TPE behaviour with maximum strains larger than 500% (Figure 4A) and a Yield strain near 3% (inset in Figure 4A and Figure 4B). The CNT/SEBS composites show different mechanical properties as a function of the surfactant used and the CNT/surfactant combination seems to affect the mechanical properties to a higher extent than the CNT content[14, 29, 31].

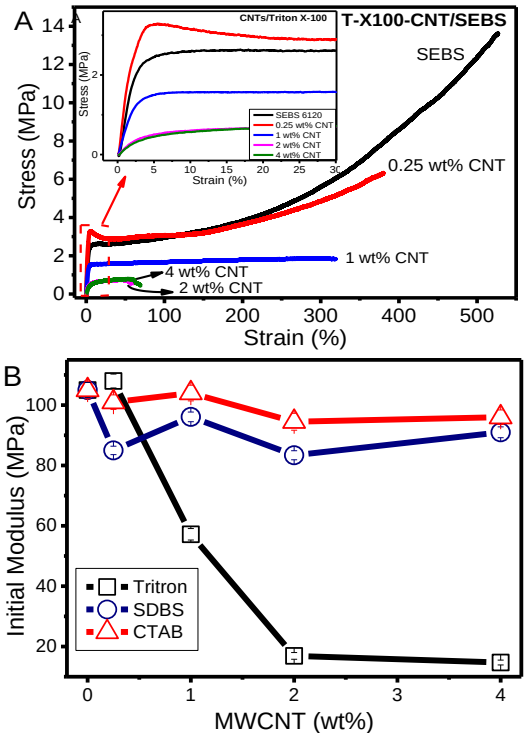

Figure 4 Stress-strain behaviour of the CNT/SEBS composites prepared using A) TX-100 as surfactant. B) Initial modulus for CNT/SEBS composites with increasing CNT content.

When using SDBS and CTAB as surfactants the mechanical properties are not significantly affected. The stress-strain curves being similar for the different composites and the maximum strain varying from 400 to 800% with similar maximum stress and Yield point values (≈3%) (Figure S3). CNT/SEBS composites without surfactants shows similar behaviour compared to composites with CTAB and SBDS surfactants[28], for similar CNT contents. On the contrary, the use of TX-100 as a surfactant decreases the mechanical properties with increasing surfactant and CNT contents. The maximum strain for composites with 0.25 wt% CNT is similar than that of neat SEBS, but with the increase in the CNT content, the maximum strain decreases for near 60% for composites with 2 and 4 wt% CNT (Figure 4A). The mechanical behaviour for composites with 2 wt% CNT and different CNT/surfactant ratio (1:1 and 1:2) is similar than that of the composite with 2:1 ratio (Figure S3 for CTAB and SDBS). Due lower properties for larger TX-100 content in CNT/SEBS composites, the mechanical properties will not improve with larger TX-100 ratio. According to the FTIR results, TX-100 was bound to the surface of CNT to a higher extent when comparing with the other surfactants used and this fact probably influences the mechanical properties of the composites. The CNT dispersion does not seem to be affected by the type of surfactant used, as observed in the SEM images. Thus, the decrease in the mechanical properties of the composites may be related to surfactant/SEBS interactions. TX-100 is a nonionic surfactant with a hydrophobic tail that has strong hydrophobic interactions with the CNT surface, leading to a higher adsorption of the surfactant as observed by FTIR and a good CNT dispersion. However, the hydrophilic coil is less compatible with the chemical structure of SEBS than the coil of the other two surfactants that possess a long hydrocarbon chain. Thus, the chemical structure of the surfactants plays a relevant role on the mechanical properties of the composites due to hydrophobic/hydrophilic interactions.

3.4 Dielectric Properties

The dielectric properties of the composites with varying CNT content and surfactant type are presented in Figure 5. The dielectric constant decreases with increasing frequency (Figure 5A) and the dielectric properties (ε' and tg δ) of the materials depend on the surfactant, increasing with increasing CNT content (Figure 5B).

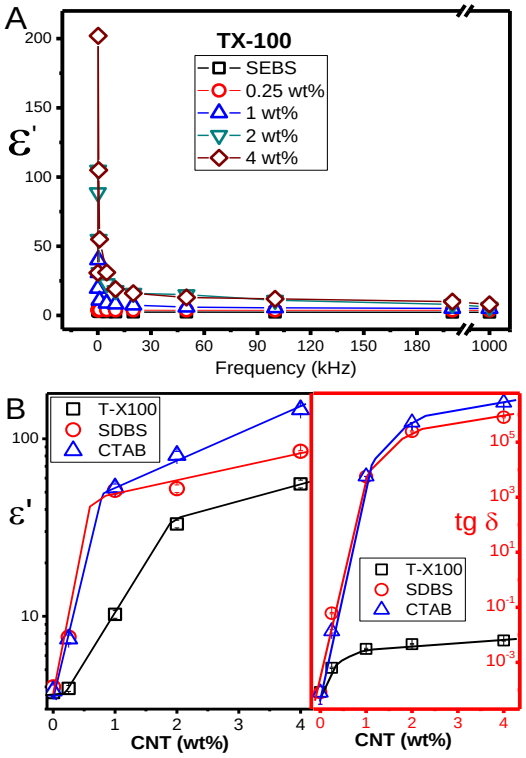

Figure 5 Dielectric properties of the CNT/SEBS composites A) in function of the frequency for CNT/SEBS composites with TX-100 surfactant and B) with three surfactants (TX-100, CTAB and SDBS) at 1 kHz.

The dielectric properties of the CNT/SEBS composites are affected by the type of surfactant used in each case. For lower CNT contents, the dielectric constant shows a small increase and the losses increase between 1 and 3 orders of magnitude for TX-100 and SDBS/CTAB surfactants, respectively. Above this concentration, the dielectric behaviour is strongly dependent on the surfactant nature. Composites with TX-100 present a gradual increase on the dielectric constant with CNT content (up to ε'≈ 55 for composites with 4 wt% CNT), but the dielectric losses value stabilizes after 1 wt% CNT content, smaller than tg δ< 0.007.

The CTAB and SDBS surfactant have less influence in the dielectric properties of the composites compared to TX-100 as the behaviour is similar to that of CNT/SEBS composites without surfactants [29, 36]. The dielectric losses increase 10 orders of magnitude from SEBS to composite with 4 wt% CNT and CTAB, and the dielectric constant increases above ε'>100. For SDBS, the dielectric constant and losses increase with increasing CNT content up to ε'≈80 and tg δ≈ 1x10^6 for composite with 4 wt% CNT.

TX-100 can be an interesting surfactant for specific applications of CNT/polymer composites, such as capacitors and energy storage systems, as the losses are still low when the dielectric constant increases. TX-100 may reduce the CNT-CNT interfaces, decreasing the dielectric response of the composites, comparing with other surfactants [29]. CTAB and SDBS show lower influence on the dielectric properties of CNT/polymer properties when compared to analogous pristine composites, with high dielectric losses and dielectric constant [37].

The electrical conductivity of the composites is presented in Figure 6. The linear current/voltages curves as a function of CNT content for TX-100 surfactant are shown in Figure 6A. Related to the dielectric response, similar electrical behaviour is obtained for composites prepared with CTAB and SDBS, and a different behaviour is obtained for TX-100 (Figure 6B).

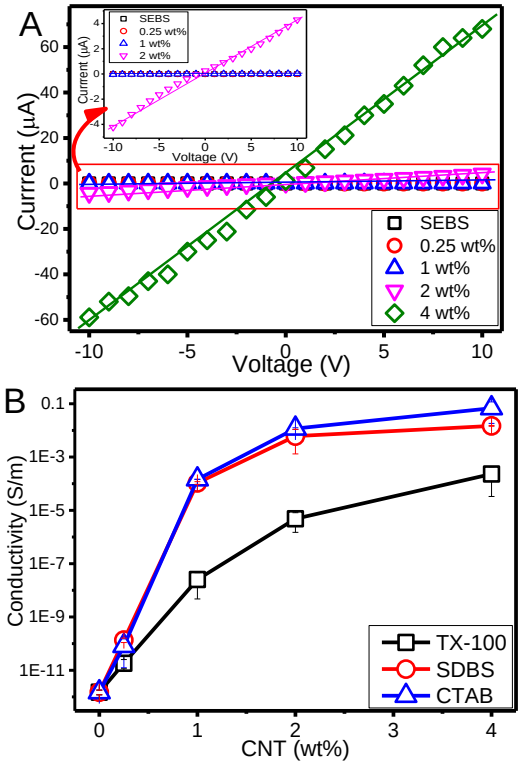

Figure 6 Current/voltage curves for CNT/SEBS composites as a function of filler content A) and B) electrical conductivity behaviour measurements for CNT/SEBS composites as a function of CNT content.

The electrical conductivity increases with CNT content regardless of the surfactant used. CTAB and SDBS surfactants show the same electrical conductivity behaviour whereas the nonionic surfactant (TX-100) has a strong influence in the electrical properties of the composites, decreasing the electrical conductivity when compared to other surfactants, or even composites without surfactant [31, 38, 39]. It was observed that anionic and cationic surfactants practically do not influence the electrical properties of the composites [14, 29, 39]. Although in terms of CNT dispersion the surfactant effect is similar for the three surfactants used in this study, the mechanical, dielectric and electrical properties are strongly affected by the use of TX-100 in CNT/SEBS composites. The addition of TX-100 decreases the electrical conductivity, dielectric constant and losses as well the mechanical properties of the composites, compared to pristine composites [14, 29] or using other surfactants such as SDBS or CTAB. This behaviour could be the result of having an isolated layer of surfactant around CNT, which can abruptly decrease the electrical conductivity of the composites while the intrinsic properties of CNT are preserved when using anionic or cationic surfactants [40].

The percolation threshold in the CNT/SEBS composites is between 0.5 to 1 wt% CNT for the different composites [29]. The surfactant nature and CNT/surfactant ratios do not affect the electrical conductivity of the composites significantly, for CTAB and SDBS surfactants. The percolation threshold increases and maximum conductivity (for 4 wt% CNT) decrease for TX-100 surfactant. This fact indicates that the use of surfactants in composite formulations results in a better cluster distribution (with lower cluster size compared to composites with CNT [29]) and that the type of surfactant also influences the electrical response of the composites, a larger effect being observed when using TX-100 as surfactant.

3.5 Piezoresistive Response

Due to the interesting mechanical properties of SEBS, composites with appropriate CNT content and conductivity values are known to present piezoresistive properties from low to large deformations [14, 29]. For CNT/SEBS composites with TX-100 surfactant the poor mechanical properties (Figure 4) for larger fillers content and low conductivity (Figure 6) compared to other surfactants, the applicability of these materials is limited for larger strain sensors materials. In this way, for larger piezoresistive sensor applications we only used CTAB and SDBS as surfactants. Figure 7 shows the piezoresistive behavior of the composites with CTAB and SDBS surfactants for several cycles at 10% strain. Typical piezoresistive behavior for 10 and 100 cycles is shown in Figures 7A and 7B. Figure 7C shows the linearity between resistance and deformation variation and piezoresistive sensibility, respectively, from 1 to 10% of strain.

Journal of Materials Chemistry A

ARTICLE

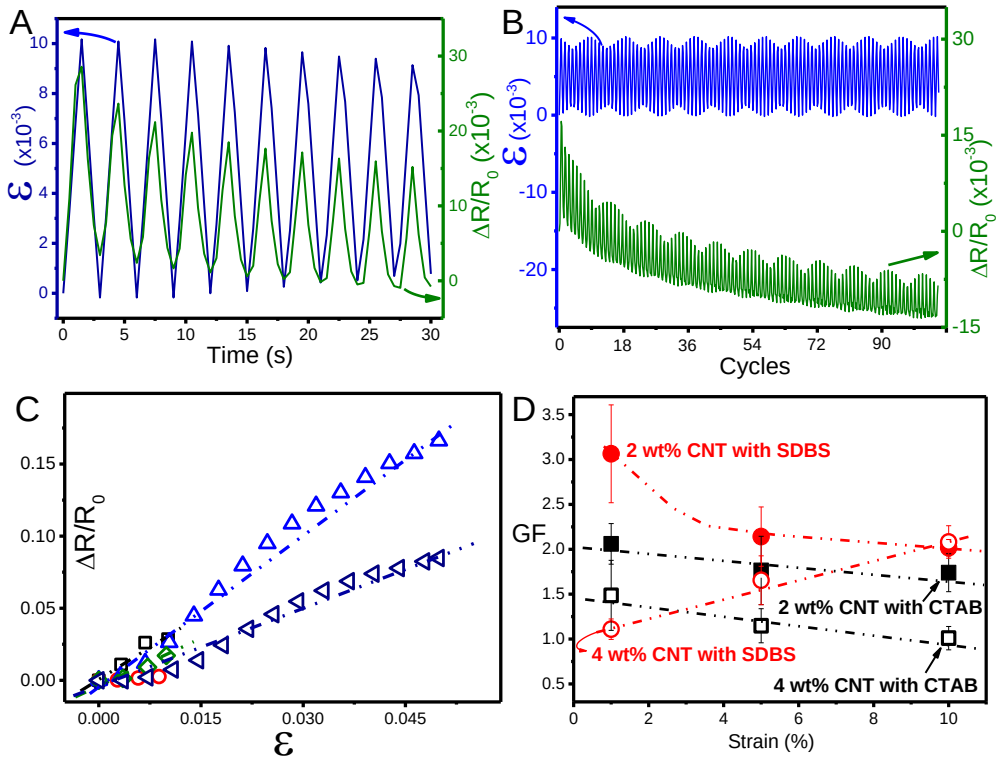

Figure 7 Piezoresistive measurements in composites with 2 and 4 wt% CNT and CTAB and SDBS as surfactants. A) representative measurements for 10 cycles for SDBS-CNT/SEBS with 2 wt% CNT and B) piezoresistive behaviour for 100 cycles with 1% strain at 5 mm/min for CTAB-CNT/SEBS with 4 wt% CNT. C) relative resistance variation as a function of the applied deformation variation from low to large deformation and D) the GF values of the composite materials.

From the piezoresistive measurements, a good linearity between the electrical and mechanical behaviour is observed. The electrical resistance changes following the loading-unloading cycles, increasing when the composite is stretched and recovering when the composite returns to the initial point. This linearity is illustrated in Figure 7D.

The composites with 2 wt% CNT (for both surfactants) show larger GF than composites with higher filler contents, being in the order of GF reported for piezoresistive composites without surfactant[28]. This phenomenon is in agreement with the percolation threshold theory. Composites with CNT content near the percolation threshold show larger piezoresistive sensibility than composites far from the threshold [22, 41], because the conductivity changes more with minor mechanical strains. The piezoresistive sensibility changes between 1< GF < 3, for composites with 2 and 4 wt% CNT and CTAB or SDBS surfactants. Composites with 4 wt% CNT have a GF lower than 2 that can be attributed to the geometric piezoresistive response (1+2v). Higher filler and surfactant contents diminish the intrinsic conductivity variation, or the CNT-CNT connectivity, under load-unload cycles. Composites with 2 wt% CNT show larger GF, near 2 for CTAB and between 3 and 2 for SDBS. These two composites can be used as piezoresistive sensors with good piezoresistive linearity. The low diameter of the CNT agglomerates in composites could be crucial, for example, in printing applications due to the micrometric size of nozzles.

The piezoresistive values of the composites with surfactants can be compared to composites materials without surfactant where the GF changes from 1 to 3 [29]. On the other hand, the decrease of the agglomerates is a required step for the production of inks for printing technologies [5] and the composites maintain a suitable piezoresistive response similar to commercial strain gages (2< GF < 5 [29]), with improved stretchability and processability for large area and high deformation applications. Thus, we can tailor polymer-based composites with piezoresistive properties comparable to commercially available ones, but with larger mechanical properties and that could be used in a wide range of printing techniques. Moreover, with CTAB or SDBS as surfactant, the clusters of CNT decrease their diameter compared with materials without surfactant [29], maintaining their interesting piezoresistive behaviour, using similar fillers contents.

4. Conclusions

Stretchable polymers with carbon nanotubes as reinforcements result in nanocomposites with excellent properties for sensing applications. CNT/SEBS composites can be tailored in view of the target applications, from low to larger strain sensors. CNT, due to van der Walls forces, tends to agglomerate in nanocomposites and CNT dispersion can be enhanced using surfactants. In this work, cationic, anionic or nonionic surfactants influence the dispersion, decreasing the diameter of CNT clusters from 5 µm in composites without surfactant to individual CNT dispersion with the three different surfactants (CTAB, SDBS and TX-100). The use of TX-100 affected the mechanical, electric and dielectric properties of the composites. The maximum strain decreased from 800% for SEBS to ≈60% in TX-100-CNT/SEBS composites and, thus, these materials resulted to be less compelling for larger strain applications. The electrical conductivity and the dielectric constant also decrease, with losses being lower up to 4 wt% CNT in the composites. On the other hand, CTAB and SDBS, showed improved CNT dispersion and low percolation threshold. The GF values change from 1 to 3, in composites with 2 and 4 wt% CNT, for both surfactants, CTAB and SDBS, and, having interesting mechanical and piezoresistive properties from low to larger strain applications. The use of CTAB and SDBS surfactants decrease the size of the agglomerates in CNT/SEBS composites while maintaining their piezoresistive behaviour, which is comparable to composites without surfactant and commercial strain gages. The improved filler dispersion promotes the use of new range of printing techniques application to this type of composites with good mechanical properties and piezoresistive behaviour.

Conflicts of interest

"There are no conflicts to declare".

Acknowledgments

This work was supported by the Portuguese Foundation for Science and Technology (FCT) in the framework of the Strategic Funding UID/FIS/04650/2013. The authors thank the FCT for financial support under projects PTDC/EEI-SII/5582/2014 and PTDC/CTM-ENE/5387/2014. P. C. also thank the FCT for the SFRH/BPD/110914/2015 grant, as well POCH and European Union. Financial support from the Basque Government Industry Department under the ELKARTEK and HAZITEK program is also acknowledged as well as funding by the Spanish Ministry of Economy and Competitiveness (MINECO) through the project MAT2016-76039-C4-3-R.

Notes and references

1. H. Deng, L. Lin, M. Z. Ji, S. M. Zhang, M. B. Yang and Q. Fu, *Prog Polym Sci*, 2014, **39**, 627-655.
2. H. Pang, L. Xu, D. X. Yan and Z. M. Li, *Prog Polym Sci*, 2014, **39**, 1908-1933.
3. D. Roy, J. N. Cambre and B. S. Sumerlin, *Prog Polym Sci*, 2010, **35**, 278-301.
4. A. Alam, Y. J. Zhang, H. C. Kuan, S. H. Lee and J. Ma, *Prog Polym Sci*, 2018, **77**, 1-18.
5. J. Oliveira, V. Correia, H. Castro, P. Martins and S. Lanceros-Mendez, *Additive Manufacturing*, 2018, **21**, 269-283.
6. K. K. Sadasivuni, D. Ponnamma, S. Thomas and Y. Grohens, *Prog Polym Sci*, 2014, **39**, 749-780.
7. L. H. Wang and J. Li, *Sensor Actuat a-Phys*, 2014, **216**, 214-222.
8. R. Costa, J. Silva and S. L. Mendez, *Compos Part B-Eng*, 2016, **93**, 310-316.
9. G. Zhang, F. Wang, J. Dai and Z. Huang, *Materials*, 2016, **9**, 92.
10. C. Lozano-Pérez, J. V. Cauich-Rodríguez and F. Avilés, *Composites Science and Technology*, 2016, **128**, 25-32.
11. H. Deng, L. Lin, M. Ji, S. Zhang, M. Yang and Q. Fu, *Prog Polym Sci*, 2014, **39**, 627-655.
12. E. Kymakis and G. A. J. Amaratunga, *J Appl Phys*, 2006, **99**.
13. P. Costa, S. Ribeiro and S. Lanceros-Mendez, *Composites Science and Technology*, 2015, **109**, 1-5.
14. P. Costa, J. Silva, V. Sencadas, R. Simoes, J. C. Viana and S. Lanceros-Mendez, *J Mater Sci*, 2013, **48**, 1172-1179.
15. N. T. Selvan, S. B. Eshwaran, A. Das, K. W. Stockelhuber, S. Wiessner, P. Potschke, G. B. Nando, A. I. Chervanyov and G. Heinrich, *Sensor Actuat a-Phys*, 2016, **239**, 102-113.
16. S. J. Chen, C. Y. Qiu, A. H. Korayem, M. R. Barati and W. H. Duan, *Powder Technol*, 2016, **301**, 412-420.
17. P. Castell, M. Cano, W. K. Maser and A. M. Benito, *Composites Science and Technology*, 2013, **80**, 101-107.
18. R. Rastogi, R. Kaushal, S. K. Tripathi, A. L. Sharma, I. Kaur and L. M. Bharadwaj, *Journal of colloid and interface science*, 2008, **328**, 421-428.
19. A. Mohamed, T. Ardyani, S. A. Bakar, P. Brown, M. Hollamby, M. Sagisaka and J. Eastoe, *Advances in colloid and interface science*, 2016, **230**, 54-69.
20. Y. Geng, M. Y. Liu, J. Li, X. M. Shi and J. K. Kim, *Compos Part a-Appl S*, 2008, **39**, 1876-1883.
21. S. Chatterjee, M. Castro and J. F. Feller, *Sensor Actuat B-Chem*, 2015, **220**, 840-849.
22. K. M. Liew, M. F. Kai and L. W. Zhang, *Compos Part a-Appl S*, 2016, **91**, 301-323.
23. Y. Bai, D. Lin, F. Wu, Z. Wang and B. Xing, *Chemosphere*, 2010, **79**, 362-367.
24. M. Shimizu, S. Fujii, T. Tanaka and H. Kataura, *J Phys Chem C*, 2013, **117**, 11744-11749.
25. B. Sohrabi, N. Poorgholami-Bejarpasi and N. Nayeri, *The journal of physical chemistry. B*, 2014, **118**, 3094-3103.
26. O. V. Kharissova, B. I. Kharisov and E. G. D. Ortiz, *Rsc Adv*, 2013, **3**, 24812-24852.
27. B. F. Gonçalves, J. Oliveira, P. Costa, V. Correia, P. Martins, G. Botelho and S. Lanceros-Mendez, *Composites Part B: Engineering*, 2017, **112**, 344-352.
28. B. F. Gonçalves, P. Costa, J. Oliveira, S. Ribeiro, V. Correia, G. Botelho and S. Lanceros-Mendez, *Journal of Polymer Science Part B: Polymer Physics*, 2016, **54**, 2092-2103.
29. B. F. Gonçalves, P. Costa, J. Oliveira, S. Ribeiro, V. Correia, G. Botelho and S. Lanceros-Mendez, *Journal of Polymer Science Part B: Polymer Physics*, 2016, DOI: 10.1002/polb.24118, n/a-n/a.
30. J. Li, P. C. Ma, W. S. Chow, C. K. To, B. Z. Tang and J.-K. Kim, *Advanced Functional Materials*, 2007, **17**, 3207-3215.
31. P. Costa, J. Silva, A. Anson-Casaos, M. T. Martinez, M. J. Abad, J. Viana and S. Lanceros-Mendez, *Compos Part B-Eng*, 2014, **61**, 136-146.
32. A. Sobolkina, V. Mechtcherine, V. Khavrus, D. Maier, M. Mende, M. Ritschel and A. Leonhardt, *Cement Concrete Comp*, 2012, **34**, 1104-1113.
33. M. Nadler, T. Mahrholz, U. Riedel, C. Schilde and A. Kwade, *Carbon*, 2008, **46**, 1384-1392.
34. T. Zhou, Z. Y. Wu, Y. Y. Li, J. A. Luo, Z. G. Chen, J. K. Xia, H. W. Liang and A. M. Zhang, *Polymer*, 2010, **51**, 4249-4258.
35. L. F. Calheiros, B. G. Soares and G. M. O. Barra, *Synthetic Met*, 2017, **226**, 139-147.
36. S. K. Yadav, S. S. Mahapatra and J. W. Cho, *J Appl Polym Sci*, 2013, **129**, 2305-2312.
37. M. L. C. Mazzucco, M. S. Marchesin, E. G. Fernandes, R. A. Da Costa, J. Marini, R. E. S. Bretas and J. R. Bartoli, *J Compos Mater*, 2016, **50**, 771-782.
38. G. Matzeu, A. Pucci, S. Savi, M. Romanelli and F. Di Francesco, *Sensor Actuat a-Phys*, 2012, **178**, 94-99.
39. X. P. Wang, Y. L. Li, J. Pionteck, Z. Zhou, W. Weng, X. G. Luo, Z. Y. Qin, B. Voit and M. F. Zhu, *Sensor Actuat B-Chem*, 2018, **256**, 896-904.
40. S. Azoz, L. M. Gilbertson, S. M. Hashmi, P. Han, G. E. Sterbinsky, S. A. Kanaan, J. B. Zimmerman and L. D. Pfefferle, *Carbon*, 2015, **93**, 1008-1020.
41. A. Ferrreira, J. G. Rocha, A. Ansón-Casaos, M. T. Martínez, F. Vaz and S. Lanceros-Mendez, *Sensors and Actuators A: Physical*, 2012, **178**, 10-16.